Molecular Cell, Volume *77*

Supplemental Information

c-di-GMP Arms an Anti-σ to Control Progression of Multicellular Differentiation in *Streptomyces*

Kelley A. Gallagher, Maria A. Schumacher, Matthew J. Bush, Maureen J. Bibb, Govind Chandra, Neil A. Holmes, Wenjie Zeng, Max Henderson, Hengshan Zhang, Kim C. Findlay, Richard G. Brennan, and Mark J. Buttner

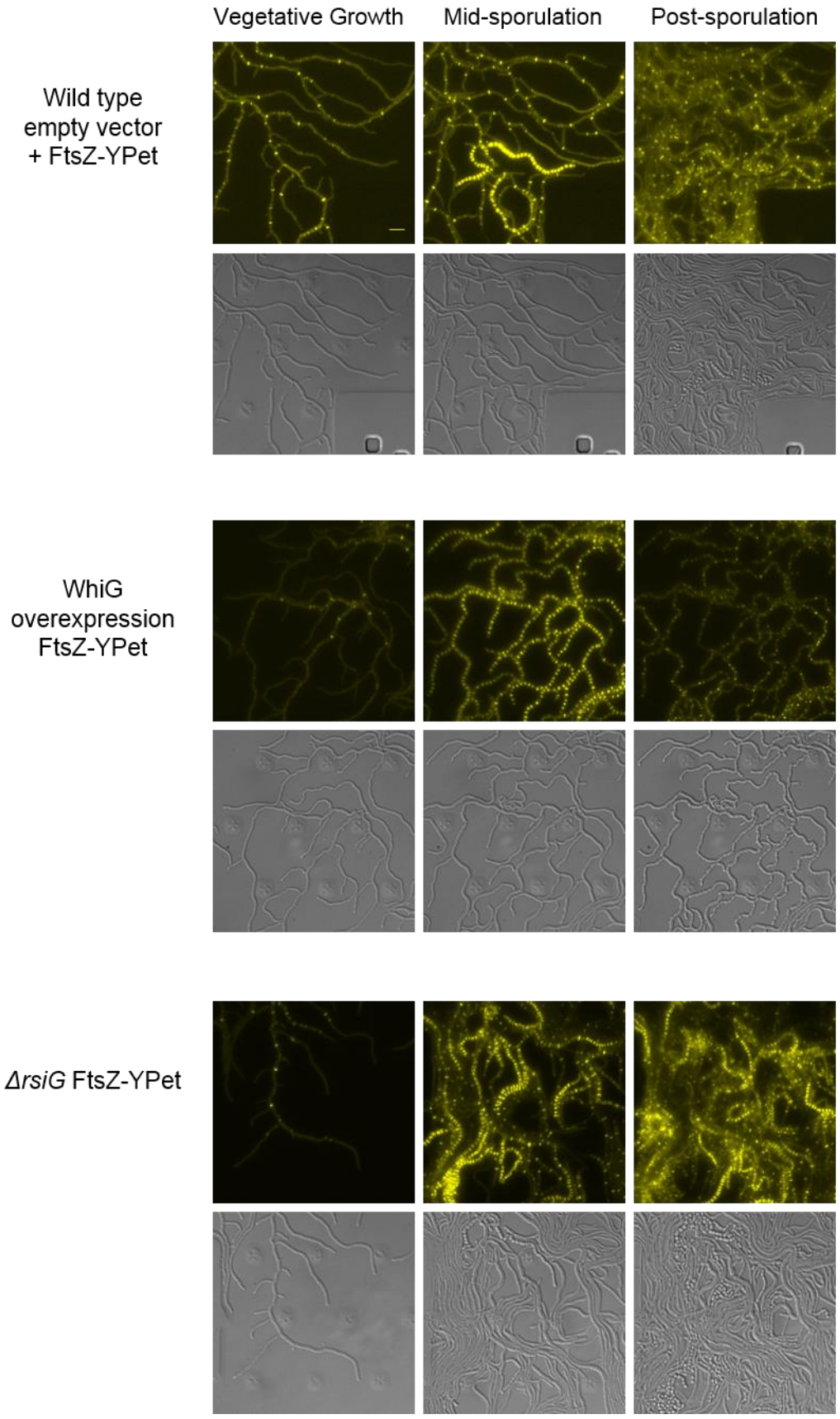

Figure S1. Overexpression of *whiG* or deletion of *rsiG* causes hypersporulation during growth in liquid culture, related to Figure 1 and Figure 4. Fluorescence (top) and DIC images (bottom) are stills taken from Movies S1-3. Scale bar = 5um.

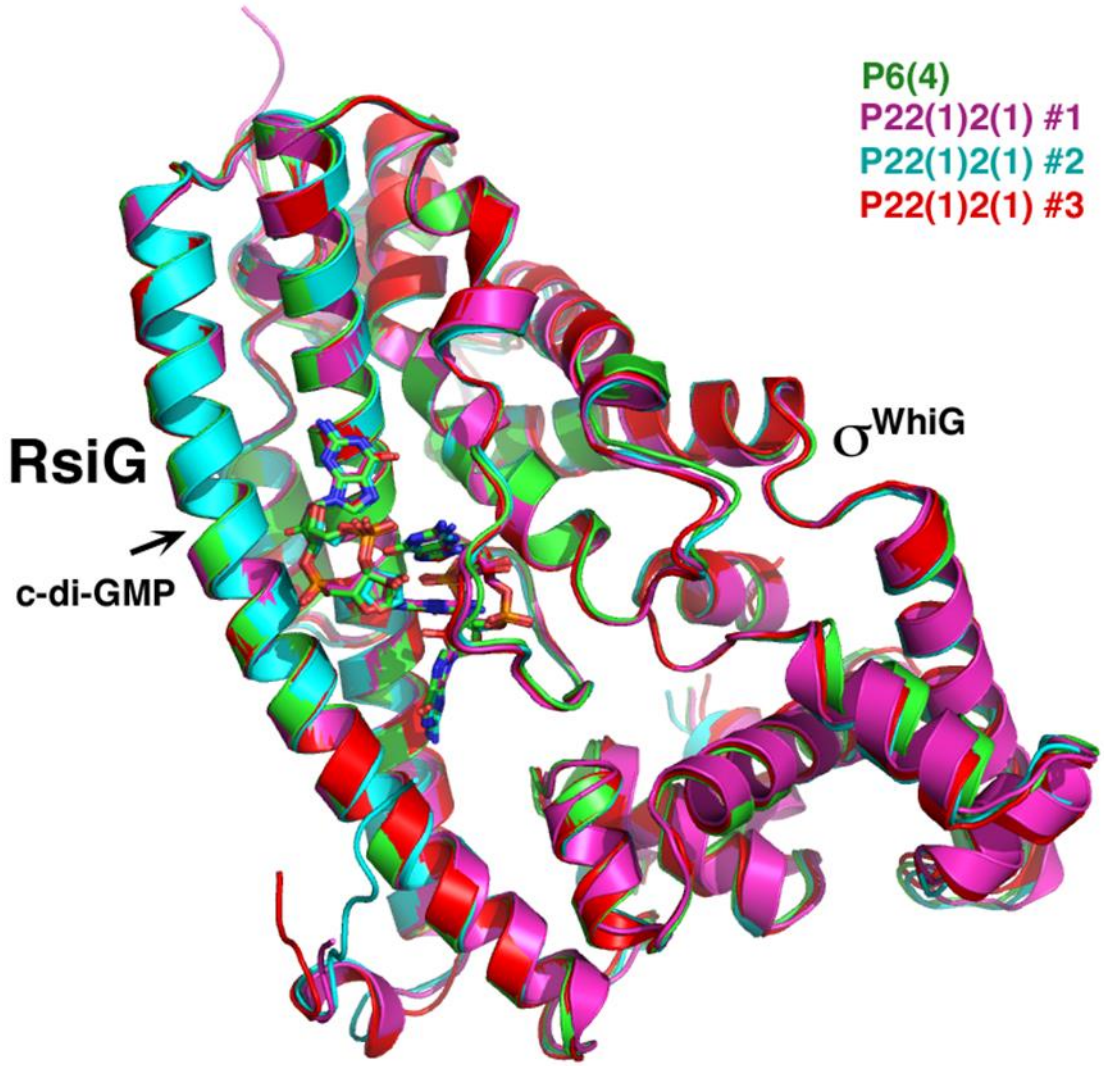

Figure S2. Superimposition of the two RsiG-σ^{WhiG} structures, related to Figure 5. The one complex in the crystallographic asymmetric unit (ASU) from the 2.08 Å structure (the hexagonal crystal form) is colored green and the three complexes in the ASU from the 3.0 Å structure (the orthorhombic crystal form) are colored magenta, cyan and red. RsiG and σ^{WhiG} are labelled as is the c-di-GMP dimer bound between the proteins. All heterodimeric complexes are identical. Also, note, each c-di-GMP dimer adopts an identical conformation when bound to the RsiG-σ^{WhiG} complex.

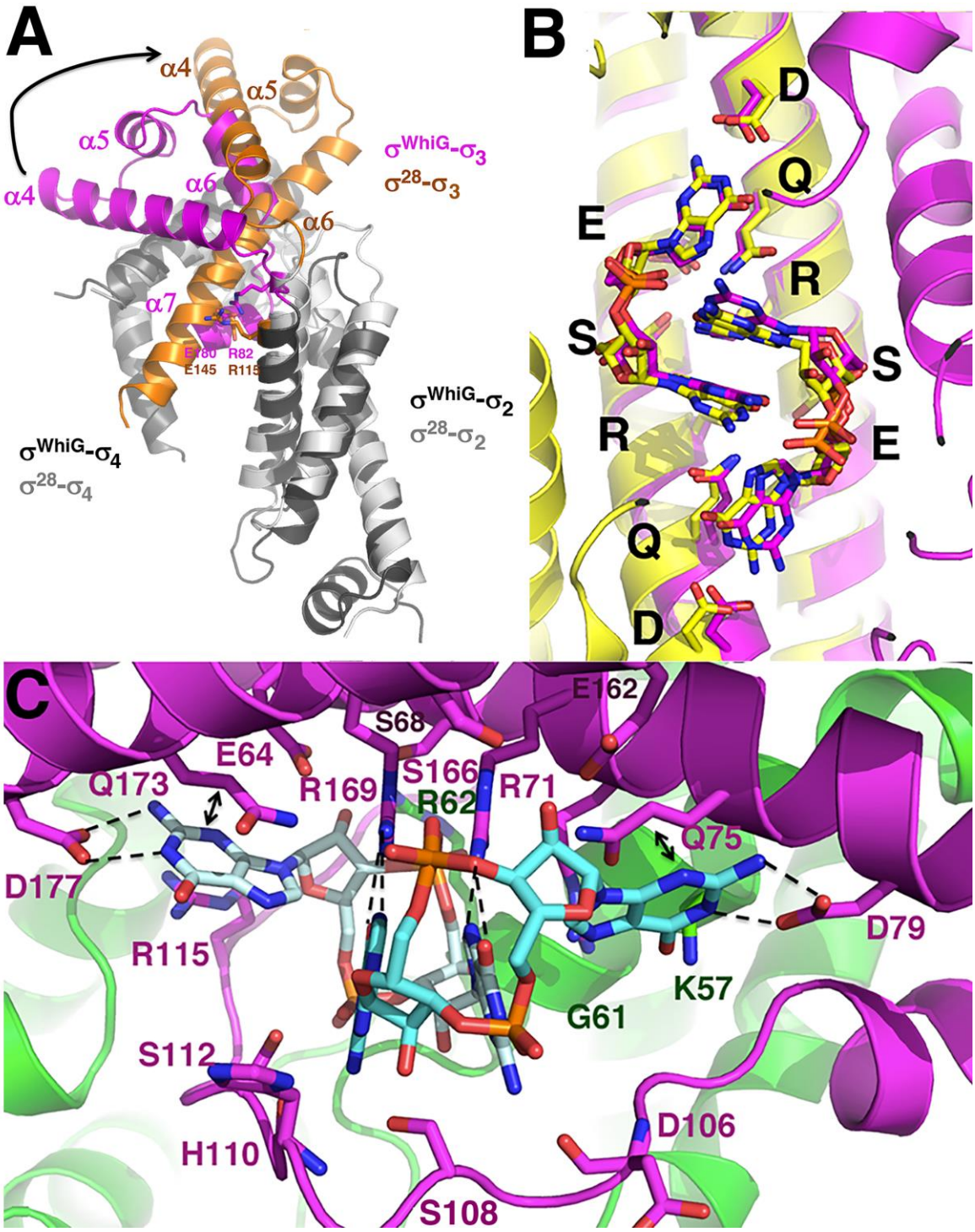

Figure S3. Characterization of RsiG and σ^{WhiG} structure and detailed interactions, related to Figure 5. (A) Overlay of the RsiG bound σ^{WhiG} structure onto the FlgM bound σ^{28} structure (Sorenson et al., 2004). σ domains 2 and 4 are colored grey and black for σ^{28} and σ^{WhiG}, respectively. These domains overlay as a unit while the σ_3 regions (colored orange and magenta σ^{28} and σ^{WhiG}, respectively) do not. Nonetheless a salt bridge is conserved between a conserved glutamate in σ_3 and conserved arginine in σ_2 of both proteins. (B) Superimposition of two RsiG structures whereby one $E(X)_3S(X)_2R(X)_3Q(X)_3D$ repeat motif of one structure (magenta) was overlaid onto the second repeat of the other structure (yellow). The remaining helices and motifs of the two structures also superimpose as do the c-di-GMP dimers. (C) Detailed c-di-GMP interactions with RsiG and σ^{WhiG}. All residues that contact c-di-GMP are shown in the figure. H-bonds are indicated by dashed lines.

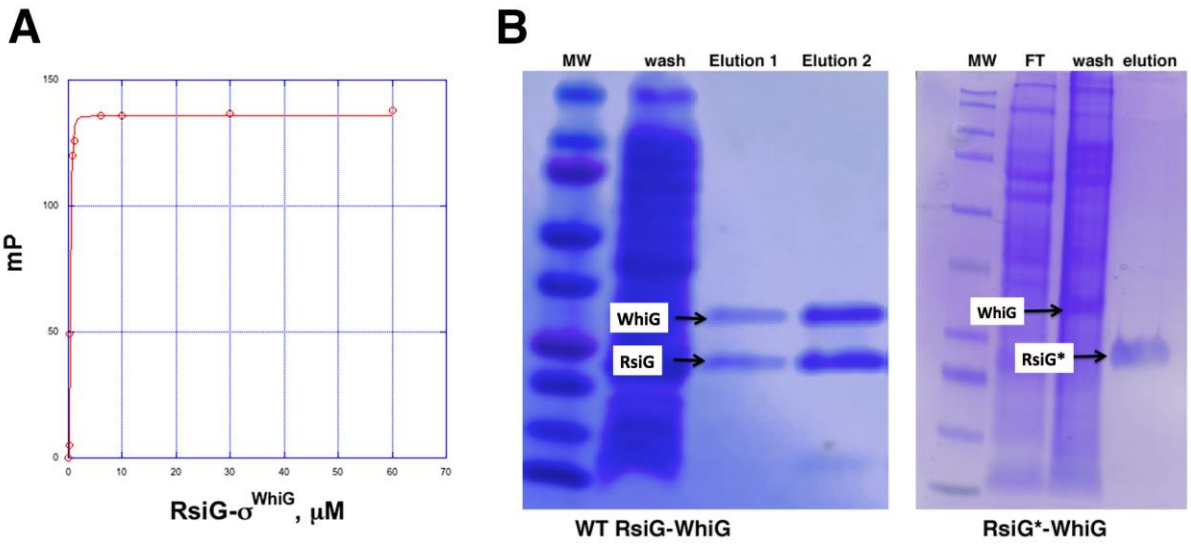

Figure S4. c-di-GMP binds with high affinity to RsiG- RsiG-σ^{WhiG} and is required for stable RsiG-σ^{WhiG} complex formation, related to Figure 7. (A) FP binding isotherm of the interaction between F-c-di-GMP and a solution with equimolar RsiG and σ^{WhiG}. The resultant K_d is 0.39 ± 0.05 μM. This experiment was repeated three times (technical replicates). (B) Coexpression of σ^{WhiG} with WT his_6-RsiG (left) or his_6-RsiG* (right). The positions of the proteins on the gel are labelled and, as can be observed, σ^{WhiG} copurifies with WT his_6-RsiG but not with his_6-RsiG*.

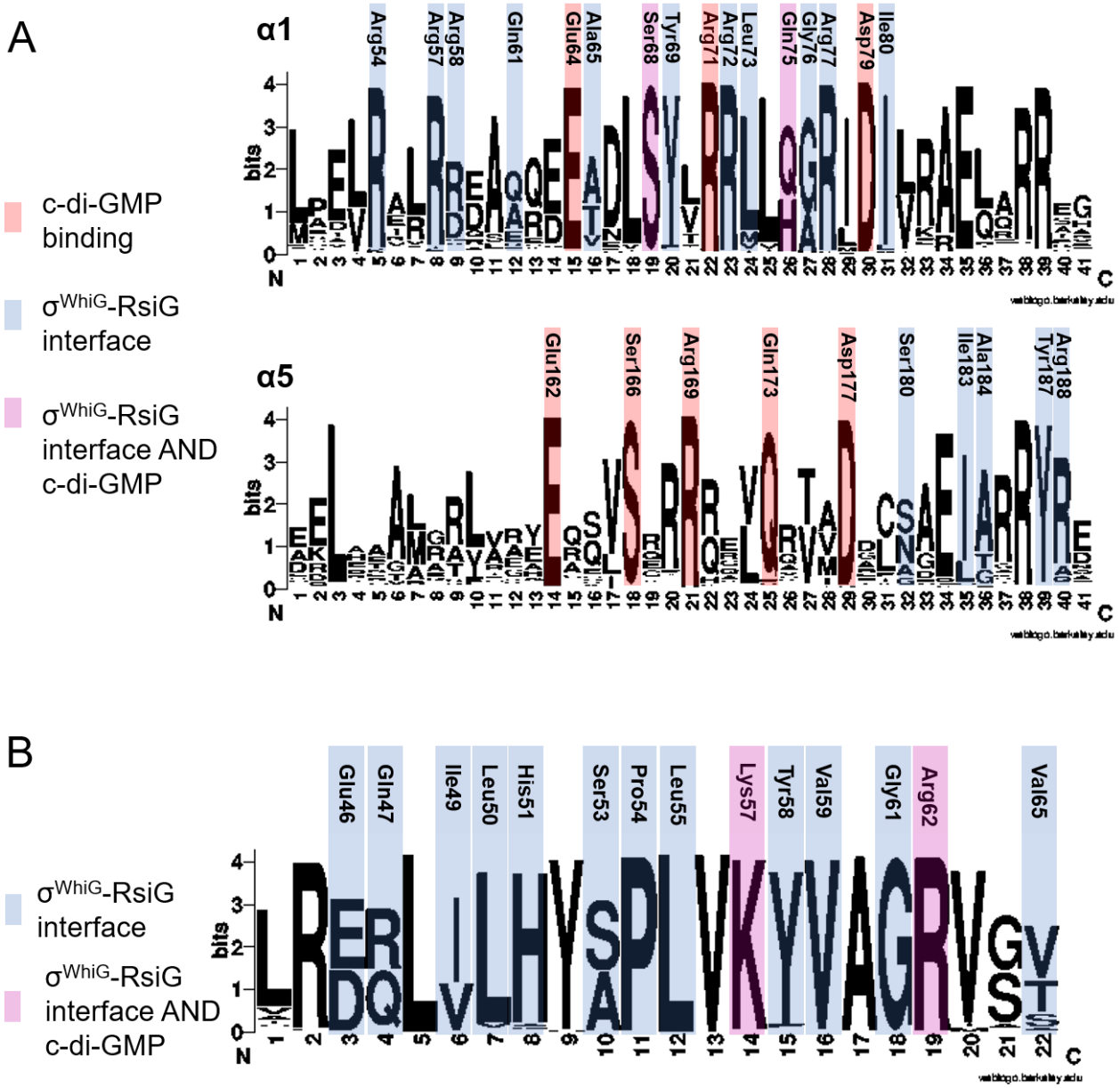

Figure S5. Conservation of residues in RsiG and σ^{WhiG} involved in binding c-di-GMP, related to Figure 7. (A) Sequence logos depicting amino acid sequence conservation of the two alpha helices involved in c-di-GMP binding among RsiG homologs in all bacteria. Residues involved in the σ^{WhiG}-RsiG interface and/or c-di-GMP binding are indicated. Note the conservation of the two $E(X)_3S(X)_2R(X)_3Q(X)_3D$ signature c-di-GMP-binding motifs. Residues are numbered based on the *S. venezuelae* sequence. RsiG homologs were identified by a reciprocal BLAST search (e-value cut off = 0.001) of the 3,962 'reference' or 'representative' annotated genomes available at GenBank, using the *S. venezuelae* RsiG sequence as a query. Homologs were aligned using MUSCLE (Edgar 2004). Fourteen sequences (all <41% sequence identity) that did not align well were removed from the analysis. The remaining 134 sequences were re-aligned, the regions of interest extracted, and the resulting alignments were used to create Weblogos (Crooks et al., 2004). (B) Sequence logo depicting amino acid sequence conservation of σ region 2.1 among σ^{WhiG} homologs that co-occur with RsiG. Residues involved in the σ^{WhiG}-RsiG interface and/or c-di-GMP binding are indicated. Note that the two σ^{WhiG} residues that make direct contacts to c-di-GMP, Lys57 and Arg62, are highly conserved. Residues are numbered based on the *S. venezuelae* sequence. Homologs were identified by a reciprocal BLAST search of the 134 genomes that contain a *rsiG* homolog, using the *S. venezuelae* σ^{WhiG} sequence as a query. The sequences were aligned using MUSCLE (Edgar 2004), σ region 2.1 was extracted and the resulting alignment used to create a Weblogo (Crooks et al., 2004).

Table S1: Data collection and refinement statistics for RsiG-σ^{WhiG} structures, related to Figures 5 and 6

Structure	form 1:RsiG-σ^{WhiG}	form 2:RsiG-σ^{WhiG}
PDB code	6PFJ	6PFV
Space group	$P6_4$	$P22_12_1$
Cell constants (Å)	a=b=92.1,c=96.6	a=79.8, b=97.3, c=204.6
Cell angles (º)	$\alpha=\beta=90.0$, $\gamma=120.0$	$\alpha=\beta=\gamma=90.0$
Resolution (Å)	79.8-2.08	87.9-3.00
R_{sym}(%)[a]	5.1 (86.9)[b]	9.8 (99.8)
R_{pim} (%)	1.4 (62.4)	5.3 (65.3)
Overall I/σ(I)	20.5 (1.4)	8.9 (1.2)
#Unique Reflections	53900	32724
#Total Reflections	410742	132151
% Complete	96.2 (94.0)	99.1 (99.1)
CC(1/2)	1.00 (0.537)	0.997 (0.447)
Multiplicity	7.1 (7.0)	4.0 (4.2)
Refinement Statistics		
Resolution (Å)	79.8-2.08	87.9-3.00
R_{work}/R_{free}(%)[c]	19.5/23.8	20.9/27.9
Rmsd		
Bond angles (º)	1.38	0.855
Bond lengths (Å)	0.004	0.004
Ramachandran analysis		
Favored (%/)	97.8	91.0
Disallowed(%)	0.0	0.0

[a] $R_{sym} = \Sigma\Sigma|Ihkl-Ihkl(j)|/ \Sigma Ihkl$, where Ihkl(j) is observed intensity and Ihkl is the final average value of intensity. [b] values in parentheses are for the highest resolution shell. [c] $R_{work} = \Sigma||Fobs| - |Fcalc||/\Sigma|Fobs|$ and $R_{free} = \Sigma||Fobs| - |Fcalc||/\Sigma|Fobs|$; where all reflections belong to a test set of 5% randomly selected data.

Table S2. Distribution of *rsiG* homologs in bacterial families, related to Figures 4, 5 and 6

Family	Number of *rsiG* homologs identified	Number of genomes in search set
Acidimicrobiaceae	2	3
Acidothermaceae	1	1
Actinopolysporaceae	2	2
Catenulisporaceae	1	1
Cellulomonadaceae	1	8
Conexibacteraceae	1	1
Cryptosporangiaceae	1	2
Geodermatophilaceae	16	16
Ilumatobacteraceae	1	1
Kineosporiaceae	1	1
Nocardioidaceae	1	19
Patulibacteraceae	1	1
Pseudonocardiaceae	39	46
Rubrobacteraceae	2	2
Streptomycetaceae	63	63
Thermoleophilaceae	1	1

Table S3. Primers, plasmids, and strains used in this study, related to STAR Methods

Primers	5' sequence
vnz26215_redi_F	GACCGCGCTGCGGTGCCCCCAGCAGCCCGGGGCACCGTGATTCCGGGGATCCGTCGACC
vnz26215_redi_R	TGGGCACGGCTCCACTGTACGACCGGCTCGCCCCGGTCATGTAGGCTGGAGCTGCTTC
vnz15005_redi_F	GGCGTCCGAAAGCCGGCGGAGGAAAGGAGCATGTGCATGATTCCGGGGATCCGTCGACC
vnz15005_redi_R	TCGTCTCATGCGGTCATGGCCTCATGGCCCATGGCCTCATGTAGGCTGGAGCTGCTTC
vnz19430_redi_F	CGGTGCGCCTCCGCACCGGTCGAGGGGACGAATCTGATGATTCCGGGGATCCGTCGACC
vnz19430_redi_R	ACCCGCACGCGAGTTTTTCCGGGCGCCGGGCCGCCGTCATGTAGGCTGGAGCTGCTTC
vnz26215_check_F	CGCATGCCCCAGCACACC
vnz26215_check_R	CTGCATCGTCCGGTGCTC
vnz15005_check_F	CGATCCGATGATCCGATCGGA
vnz15005_check_R	GTCGTCGATCCCCAGGTGA
vnz19430_check_F	TGCACCACTGCACGCATGC
vnz19430_check_R	GCTGCCAGTCGGGGAACTC
vnz26215_comp_F	GGCGAAGCTTCCTGGAGCATTCGGGTGA
vnz26215_comp_R	GGGGTACCGGTGCTCGGCCACCGAG
vnz19430_comp_F	GGCGAAGCTTACCCTCTGCACCACTGCAC
vnz19430_comp_R	GGGGTACCCATCCTCCGACCCTACGCAG
vnz26215_ermE_F	GGGAATTCCATATGCCCCAGCACACCTCCG
vnz26215_ermE_R	GGAAGCTTGGTGCTCGGCCACCGAG
HI_ermE_P1	GTCTAGAACAGGAGGCCCCATATGAGTACCCTTGCGCACACCATG
HI_ermE_P2	TTACCTCCGATGTTGAGTCAGTGTTCGCGGGGGGC
HI_ermE_P3	CGAACACTGACTCAACATCGGAGGTAAGCCATGTCCGTTCTCCTCGAG
HI_ermE_P4	TGAGAACCCTAGGGGATCCAAAGCTTTCAGTGGATGATC
vnz28820_qRT_F	CGGGAGGTCGAGGTGCTCAG
vnz28820_qRT_R	TGGCTCTTCACGGTGAGGGC
hrdBqRT_F	TGTTCTGCGCAGCCTCAATC
hrdBqRT_R	CTCTTCGCTGCGACGCTCTT
vnz26215_BACTH_F	CTAGTCTAGAGATGCCCCAGCACACCTCCG
vnz26215_BACTH_R	GGGGTACCCGGCGTCCGACGTCGGCCA
T18seq_F	GTGTGGAATTGTGAGCGGAT
T18seq_R	TTCCACAACAAGTCGATGCG
T25seq_F	CGGTGACCAGCGGCGATT
T25seq_R	GGCGATTAAGTTGGGTAACGCC
NT25seq_F	CCCCAGGCTTTACACTTTATGC
NT25seq_R	TTGATGCCATCGAGTACGGCT
T18Cseq_F	GTGCCGAGCGGACGTTCGA
T18Cseq_R	CTTAACTATGCGGCATCAGAGC
vnz19430_BACTH_F	GGGGTACCCGGGCGAGCAGGTCGTCGAC
vnz19430_BACTH_R	CTAGTCTAGAGATGAGTGCACCTGGCACCGG
vnz26215_MCS1_F	CCGGAATTCGATGCCCCAGCACACCTCCG
vnz26215_MCS1_R	CCCAAGCTTTCAGCGTCCGACGTCGGC
vnz19430_MCS2_F	GGGAATTCCATATGAGTGCACCTGGCACCGG
vnz19430_MCS2_R	GGGGTACCTCAGGCGAGCAGGTCGTCG

Plasmid	Relevant genotype/comments	Source
pIJ790	Modified l RED recombination plasmid [*oriR101*] [*repA101*(ts)] *araBp-gam-be-exo*	Gust et al., 2003
pIJ773	Plasmid template for amplification of the apr oriT cassette for 'Redirect' PCR-targeting	Gust et al., 2003
pIJ10770	Plasmid cloning vector for the conjugal transfer of DNA from *E. coli* to *Streptomyces* spp. Integrates site specifically at the ΦBT1 attachment site (Hyg^R).	Schlimpert et al., 2017
pIJ10900	pIJ10770 carrying *whiG* driven from its own promoter	This work
pIJ10901	pIJ10770 carrying *rsiG* driven from its own promoter	This work
pIJ10913	pIJ10770 carrying *rsiG** driven from the WT *rsiG* promoter	
pIJ10257	Plasmid cloning vector for the conjugal transfer of DNA (under control of the ermE* constitutive promoter) from *E. coli* to *Streptomyces* spp. Integrates site specifically at the ΦBT1 attachment site (Hyg^R).	Hong et al., 2005
pIJ10902	pIJ10257 carrying *whiG*, driven by ermE*	This work
pIJ10906	pIJ10257 carrying *whiH* and *whiI*, driven by ermE*	This work
pKT25	Two-hybrid plasmid, N-terminal cyaAT25 fusion (Kan^R)	Karimova et al., 1998
pKNT25	Two-hybrid plasmid, C-terminal cyaAT25 fusion (Kan^R)	Karimova et al., 1998
pUT18	Two-hybrid plasmid, C-terminal cyaAT18fusion (Amp^R)	Karimova et al., 1998

Plasmid	Relevant genotype/comments	Source
pUT18C	Two-hybrid plasmid, N-terminal cyaAT18fusion (Amp^R)	Karimova et al., 1998
pKT25-zip	A derivative of pKT25 in which the leucine zipper of GCN4 is genetically fused in frame to the T25 fragment	Karimova et al., 1998
pUT18C-zip	A derivative of pUT18C in which the leucine zipper of GCN4 is genetically fused in-frame to the T18 fragment	Karimova et al., 1998
pIJ10907	pKT25 carrying *whiG*	This work
pIJ10908	pKNT25 carrying *whiG*	This work
pIJ10909	pUT18 carrying *whiG*	This work
pIJ10910	pUT18C carrying *whiG*	This work
pIJ10911	pKT25 carrying *rsiG*	This work
pIJ10912	pUT18 carrying *rsiG*	This work
pCOLADuet-1	Expression vector for coexpression of two target genes, each under the control of a T7 promoter (Kan^R)	Novagen
pET15B	T7 expression vector (Amp^R)	Novagen
pIJ10914	pCOLADuet-1 carrying *whiG* at MCS1 and *rsiG* at MCS2	This work
pIJ10915	pCOLADuet-1 carrying Δ26 *rsiG* at MCS1 and *whiG* at MCS2 (genes codon optimized for *E. coli*)	This work
pIJ10916	pCOLADuet-1 carrying Δ26 *rsiG** at MCS1 and *whiG* at MCS2 (genes codon optimized for *E. coli*)	This work
pIJ10917	pCOLADuet-1 carrying *rsiG* at MCS1	This work
pIJ10918	pET15B carrying *rsiG** (gene codon optimized for *E. coli*)	This work
pIJ10919	pCOLADuet-1 carrying Δ26 *rsiG*(L56M-L85M) at MCS1 (gene codon optimized for *E. coli*)	This work
pIJ10920	pCOLADuet-1 carrying *whiG* at MCS1 (gene codon optimized for *E. coli)*	This work
pKF351	Plasmid cloning vector for the conjugal transfer of DNA from *E. coli* to *Streptomyces* spp. Integrates site specifically at the ΦC31 attachment site (Hyg^R) and carries *ftsZ-ypet* driven from its own promoter.	Schlimpert et al., 2017
pSS5	Plasmid cloning vector for the conjugal transfer of DNA from *E. coli* to *Streptomyces* spp. Integrates site specifically at the ΦBT1 attachment site (Hyg^R) and carries *ftsZ-ypet* driven from its own promoter.	Schlimpert et al., 2017

Strains	Relevant genotype/notes	Reference
S. venezuelae		
ATCC10712	wild type	
SV6	*ΔwhiG::apr*	This work
SV80	*Δvnz15005::apr*	This work
SV81	*ΔrsiG::apr*	This work
SV6-pIJ10770	*ΔwhiG::apr* with pIJ10770 integrated at the ΦBT1 attachment site	This work
SV6-pIJ10900	*ΔwhiG::apr* with pIJ10900 integrated at the ΦBT1 attachment site	This work
Sven-pIJ10257	wild type with pIJ10257 integrated at the ΦBT1 attachment site	This work
Sven-pIJ10902	wild type with pIJ10902 integrated at the ΦBT1 attachment site	This work
SV6-pIJ10257	*ΔwhiG::apr* with pIJ10257 integrated at the ΦBT1 attachment site	This work
SV6-pIJ10906	*ΔwhiG::apr* with pIJ10906 integrated at the ΦBT1 attachment site	This work
SV81-pIJ10770	*ΔrsiG::apr* with pIJ10770 integrated at the ΦBT1 attachment site	This work
SV81-pIJ10901	*ΔrsiG::apr* with pIJ10901 integrated at the ΦBT1 attachment site	This work
SV81-pIJ10913	*ΔrsiG::apr* with pIJ10913 integrated at the ΦBT1 attachment site	This work
Sven-pIJ10257-pKF351	wild type with pIJ10257 integrated at the ΦBT1 attachment site and pKF351 integrated at the ΦC31 attachment site	This work
Sven-pIJ10902-pKF351	wild type with pIJ10902 integrated at the ΦBT1 attachment site and pKF351 integrated at the ΦC31 attachment site	This work
SV81-pSS5	*ΔrsiG::apr* with pSS5 integrated at the ΦBT1 attachment site	This work
E. coli		
DH5α	F– ϕ80*lac*ZΔM15 Δ(*lac*ZYA-*arg*F)U169 *rec*A1 *end*A1 *hsd*R17(rK–, mK+) *pho*A *sup*E44 λ– *thi*-1 *gyr*A96 *rel*A1	Invitrogen
ET12567(pUZ8002)	ET12567 containing helper plasmid pUZ8002	Paget et al., 1999
BW25113	Δ(*araD-araB*)*567* Δ*lacZ4787*(::*rrnB-4*) *lacIp-4000*($lacI^Q$), λ−*rpoS369*(*Am*) *rph-1*Δ(*rhaD-rhaB*)*568 hsdR514*	Datsenko and Wanner 2000
BTH101	F– *cya-99 araD139 galE15 galK16 rpsL1 (Strr) hsdR2 mcrA1 mcrB1*	Karimova et al., 1998
BL21 pLysS Rosetta	F– *ompT hsd*S(rB- mB-) *gal dcm* (DE3) pLysSRARE (Cam^R)	Novagen